PHYSICAL REVIEW B VOLUME 16, NUMBER 8 15 OCTOBER 1977

Low-temperature electrical and thermal resistivities of potassium: Deviations from Matthiessen's rule*

W. D. Jumper and W. E. Lawrence
Department of Physics, Dartmouth College, Hanover, New Hampshire 03755
(Received 17 January 1977)

The low-temperature electrical and thermal resistivities of potassium are calculated as functions of temperature and impurity concentration. Realistic phonon spectra are used for computing the electron-phonon interaction. The variational calculation of the transport coefficients employs a trial distribution function which contains a nontrivial dependence on both the energy and the angular coordinates, so that deviations from Matthiessen's rule (DMR) in the electrical resistivity may be calculated to better accuracy than previously possible. Both the energy and the angular dependence are found to be relevant for the electrical resistivity, and the improved calculation gives good agreement with the experimentally observed DMR. For the thermal resistivity our results agree with previous ones; the angular dependence is found to be unimportant, and as a result we obtain essentially no improvement over calculations which use energy-dependent trial functions. The lack of agreement with the observed DMR in the thermal case tends to confirm the earlier conclusion that another mechanism is involved.

I. INTRODUCTION

The low-temperature electrical and thermal resistivities of potassium have undergone intensive study in recent years, both experimental[1-3] and theoretical.[4-12] The general temperature dependence of the electrical resistivity seems to be well understood[8] [except at the very lowest temperatures, below about 2 K (Ref. 13)], and the current questions focus on the more particular aspects such as the deviations from Matthiessen's rule (DMR), i.e., the failure of additivity between the residual and temperature-dependent resistivities. A number of possible mechanisms for this effect have been discussed; among them are phonon drag, inelastic scattering from impurities, and macroscopic defects. These mechanisms are relatively complicated and have not yielded to rigorous quantitative calculations useful for comparison with experiment. Those calculations which have yielded results that could be compared with experiment fall into the following category: the electron-impurity and electron-phonon scattering probabilities are treated as additive and independent of one another; the DMR then results from the form of the nonequilibrium distribution, which is different for one scattering mechanism from what if is for the other, when each mechanism is taken alone.

Recent calculations of the electrical resistivity employ a nontrivial angular dependence in the distribution function.[4-6] Sondheimer[14] had much earlier considered the energy dependence in a model which ignored umklapp processes and found its effect to be small. In this work we treat the two effects in combination by means of a variational expansion of the trial distribution function and within a realistic model of the electron-phonon interaction. The details of the calculation are described in Sec. II. In Sec. III we present the results which may be summarized here briefly as follows: our new result is for the electrical resistivity, where we find that the energy-dependent contribution to the total DMR is (i) comparable in magnitude with, but (ii) occurs at higher impurity concentrations than the angular-dependent contribution. As a result of these two features, we obtain an agreement with the observed DMR which was previously lacking, particularly in the ^{4}He temperature range for the less pure samples.

In the case of the thermal resistivity we have no substantially new results to report, and we can only confirm a number of previous ones. While the focus of previous work has been on the energy dependence of the distribution function,[10-12] Kus[11] has nevertheless treated the angular dependence in combination with it, using the approximation of Robinson and Dow,[15] and shown that its effect is very small. Since this approximation tends to overestimate the DMR, (as discussed in Ref. 6), it is indeed appropriate for demonstrating the small effect of the angular dependence on the thermal resistivity. It is not surprising that we find a similarly small effect with the variational method. (Since we are primarily interested in the electrical resistivity where the angular effect is large, we more appropriately use the variational method, which tends to underestimate the DMR.) We should point out that Leaven's[12] calculation is the most accurate one which exists for the thermal conductivity. Although angular dependence is ignored in his treatment, the energy dependence is calculated by numerical integration of the Boltzmann equation, and hence the clean limit is predicted

more accurately than by the variational calculations (of Refs. 10, 11, and the present work, for example). In addition the phonon spectra and form factor are calculated from first principles, although, as Leavens points out, the data do not distinguish between the first-principles phonon spectra and those calculated from a fit to neutron data.

Incidentally, we have retained up to four terms in our power-series expansions of the energy-dependent functions in order to study the accuracy of the resulting resistivities. It is interesting to compare these results (Sec. III) with those of Leaven's calculation.

II. CALCULATIONS

We begin this section by discussing the trial distribution function, since it is the new ingredient in the calculation. The deviation function $\Psi(\vec{k})$ may be introduced as usual by expanding the distribution function

$$f(\vec{k}) = f^0(E_k) - \frac{\partial f^0(E_k)}{\partial E_k}\Psi(\vec{k}) \tag{1}$$

about its equilibrium $f^0(E_k)$. The linearized Boltzmann equation then takes the form

$$X(\vec{k}) = \sum_{k} P(\vec{k},\vec{k}')[\psi(\vec{k}) - \psi(\vec{k}')], \tag{2}$$

where

$$X(\vec{k}) = -\frac{\partial f^0}{\partial E}\vec{F}\cdot\vec{v}(\vec{k}) \tag{3}$$

is the "forcing" term, with $\vec{F}$ proportional to the applied electric field $\vec{\epsilon}$ or temperature gradient $\vec{\nabla}T$, i.e.,

$$\vec{F} = \begin{cases} e\vec{\epsilon}, & \text{electrical case} \quad (4a) \\ \eta k_B \vec{\nabla}T, & \text{thermal case,} \quad (4b) \end{cases}$$

where

$$\eta = (E_k - \mu)/k_B T \tag{5}$$

is a reduced energy variable which we shall use throughout. The scattering kernel $P(\vec{k},\vec{k}')$ is the sum of electron-phonon and electron-impurity contributions

$$P(\vec{k},\vec{k}') = P_\phi(\vec{k},\vec{k}') + P_{\text{imp}}(\vec{k},\vec{k}'). \tag{6}$$

For illustrative purposes, consider first the impurity piece; its important properties are that it is elastic and, to sufficiently good approximation for our purposes, isotropic. Accordingly, it may be written

$$P_{\text{imp}}(\vec{k},\vec{k}') = (2\pi/\hbar)V_{\text{imp}}^2(|\vec{k}-\vec{k}'|)\delta(E_k - E_{k'}), \tag{7}$$

where the isotropy is expressed through the fact that the matrix element V_{imp} depends only on the magnitude of the wave-vector difference and not on the individual wave vectors themselves. If there is no electron-phonon scattering (i.e., at $T=0$), the solution of (2) is

$$\Psi(\vec{k}) = \vec{F}\cdot\vec{v}(\vec{k})\tau_{\text{imp}}, \tag{8}$$

where the electron-impurity scattering rate is

$$\tau_{\text{imp}}^{-1} = \frac{2\pi}{\hbar}N(0)\int_{-1}^{1}\frac{d(\cos\theta)}{2}(1-\cos\theta)V_{\text{imp}}^2(2k_F\sin\tfrac{1}{2}\theta)$$

$$= \frac{2\pi}{\hbar}N(0)\langle V_{\text{imp}}^2\rangle, \tag{9}$$

where $N(0)$ is the density of states of a single spin at the Fermi level, and angular brackets denote the average over the angle θ between $\vec{k}$ and $\vec{k}'$. The residual ($T\to 0$) resistivities, which are due to electron-impurity scattering alone, are just, for the electrical case,

$$\rho_0 = m/ne^2\tau_{\text{imp}}, \tag{10a}$$

and for the thermal case,

$$W_0 = W_{\text{imp}} = 3m/\pi^2 nk_B^2 T\tau_{\text{imp}}. \tag{10b}$$

Expressions (9) and (10) will be useful later since we shall have to infer the strength V_{imp}^2 of the impurity kernel from the measured residual resistivities of various samples. In computing the results to be shown in Sec. III, we have in fact simply taken $V_{\text{imp}}(\vec{k}-\vec{k}')$ to be a constant. Similar computations with other functional forms produced essentially the same results.

The electron-phonon kernel P_ϕ has neither of the properties mentioned for P_{imp}. Its inelasticity gives rise to nontrivial energy dependence of the deviation function, and its anisotropy gives rise to nontrivial angular dependence. To incorporate these into the calculation we generalize (8) by writing

$$\Psi(\vec{k}) = \vec{F}\cdot\vec{v}(\vec{k})\tau(\vec{k}), \tag{11}$$

and we then expand τ in powers of the energy variable η (5), and in Kubic harmonics of the angular variables θ and ϕ (denoted by $\hat{k}$):

$$\tau(k) = \sum_{n\ (\text{even})}\sum_{l}\tau_{nl}\eta^n K_l(\hat{k})$$

$$= \tau_{00} + \tau_{04}K_4(\hat{k}) + \tau_{06}K_6(\hat{k})$$

$$+ \eta^2[\tau_{20} + \tau_{24}K_4(\hat{k}) + \tau_{26}K_6(\hat{k})]. \tag{12}$$

The second and third lines give the actual form used in the calculation. The Kubic harmonics K_4 and K_6 are retained because these are the lowest nontrivial orders belonging to the identity representation of the cubic group, and because their combination (together with the constant τ_{00}) is cap-

able of producing a minimum in the [110] direction, while remaining large in other symmetry directions [100] and [111] which are shown in Fig. 1. This is the behavior expected (at least in the case of the electrical resistivity) on the basis of the sharp peaking of electron-phonon umklapp scattering strengths about the [110] directions.[16] The η expansion contains constant and quadratic terms in the case of the electrical resistivity; in the thermal case [owing to the form of $\vec{F}$ (4b)], linear and cubic terms are present. Generally one has even (odd) powers of η in the electrical (thermal) case, as is well known from previous studies of the energy dependence alone. In the Appendix it is shown that the same feature occurs in the present case, in which nontrivial angular dependence is included as well. We have briefly studied the effect of adding higher-order terms in the η expansion, and this will be discussed in Sec. III; it does not alter our basic conclusions.

The electron-phonon contribution to the scattering kernel is[17]

$$P_\phi(\vec{k},\vec{k}')=\frac{2\pi}{\hbar}\sum_\sigma |g_\sigma(\vec{k},\vec{k}')|^2 f^0(E_k)f^0(E_{k'})[k_BT|e^{-\eta}-e^{-\eta'}|]^{-1}[\delta(E_k-E_{k'}-\hbar\omega_\sigma)+\delta(E_k-E_{k'}+\hbar\omega_\sigma)], \tag{13}$$

where

$$|g_\sigma(\vec{k},\vec{k}')|^2=\omega_\sigma|\langle\vec{k}'|\hat{\epsilon}_\sigma\cdot\vec{\nabla}V|\vec{k}\rangle|^2 \tag{14}$$

contains the squared matrix element between single-orthogonalized-plane-wave states of an operator involving the electron-ion pseudopotential V and the phonon polarization vector $\hat{\epsilon}_\sigma$ for the mode σ. Both this and the phonon frequency ω_σ are assumed to be evaluated at wave vector $\vec{k}-\vec{k}'$ reduced to the first Brillouin zone; they are generated by means of a fifth-nearest-neighbor force-constant model, fit to inelastic neutron scattering data and sound velocity data of Cowley, Woods, and Dolling.[18] Most of the results to be shown in Sec. III were obtained using the Bardeen pseudopotential form factor.[19] To demonstrate the sensitivity of the results to the choice of the form factor, we repeated some of the calculations using the Ashcroft one.[20] These choices follow in the spirit of Refs. 4, 5, 9, and 10.

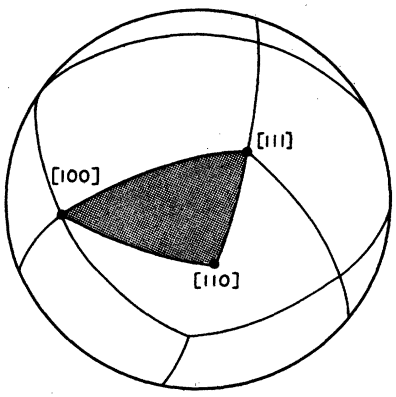

FIG. 1. Brillouin-zone edges are projected onto the Fermi surface to exhibit the face-centered-cubic structure of the reciprocal lattice. Zone corners are in the [100] and [111] directions. [110] is the direction of closest approach to the zone faces, and the location of umklapp-scattering "hot spots".

Because of the complexity of P_ϕ, the finite order expansion (12) cannot be an exact solution of (2), but the usual variational interpretation applies: a resistivity functional (to be written down shortly) is minimized with respect to the expansion parameters in (12). The minimization produces the least upper bound on the *exact* resistivity [i.e., that which would be calculated from the exact solution of (2)]. To state this concretely, we write the right-hand side of (2) as $P\Psi(\vec{k})$, and introduce the inner product of two functions $f(\vec{k})$ and $g(\vec{k})$ as the usual $\vec{k}$ space summation

$$(f,g)=2\sum_{\vec{k}} f(\vec{k})g(\vec{k})=\frac{1}{4\pi^3}\int d^3k f(\vec{k})g(\vec{k}). \tag{15}$$

Then the variational resistivity, as a functional of $\Psi(\vec{k})$, is

$$\rho\{\Psi\}=(\Psi,P\Psi)/(X,\Psi)^2 \tag{16}$$

(write W instead of ρ for the thermal case), where $\Psi(\vec{k})$ is given by (11) and (12). The minimization procedure is a straightforward extension of Sondheimer's method.[14]

For discussion and plotting purposes in Sec. III it is convenient to review the conventional notation for the various contributions to the total electrical resistivity (16):

$$\rho\{\Psi\}=\rho(T,\rho_0)=\rho_0+\rho_T=\rho_0+\rho_I+\Delta, \tag{17}$$

where $\rho_0=\rho(0,\rho_0)$ is the residual, and $\rho_T=\rho(T,\rho_0)-\rho_0$ the temperature-dependent, resisitivity; $\rho_I=\rho(T,0)$ is the ideal resistivity, and $\Delta=\rho_T-\rho_I$ is the deviation from Matthiessen's rule. Of course ρ_T and Δ are functions of both ρ_0 and the temperature, and will sometimes be written as such, e.g., $\rho_T=\rho_T(T,\rho_0)$. In the case of the *thermal* resistivity, the appropriate parameter in terms of which to describe the impurity dependence is TW_0, rather than W_0 which is (10b) inversely proportional to the

temperature. So the analog of (17) is

$$W(\Psi) = W(T, TW_0) = W_0 + W_T = W_0 + W_I + \delta \ , \qquad (18)$$

where δ is the deviation from Matthiessen's rule. Incidentally, we shall apply the terms "residual" and "temperature-dependent" to the thermal as well as the electrical resistivity, with the understanding that "residual" applies to the temperature-independent quantity TW_0 (not just W_0), which appears as an argument in (18).

III. RESULTS

We discuss first the electrical resistivity. To give a brief overview of the effects of the various trial functions, we plot resistivity versus temperature of Fig. 2 for the four choices indicated. The top curve results from the simplest trial function $\tau(\hat{k}) =$ constant and thus represents the dirty limit of the temperature-dependent resistivity, $\rho_T(T, \infty)$. The remaining curves represent improving approximations to the pure metal: in descending order, the trial functions include angular-dependence alone, energy dependence alone, and finally, the combined dependences. The effects of the two dependences are approximately additive, with angular dependence contributing slightly more than one-third of the total improvement. The difference between the top and bottom curves represents the maximum DMR $\Delta(T, \infty)$ (Eq. 17) predicted by the general trial function, and it compares well with the DMR found in the measured resistivities of Ref. 1.

A more meaningful comparison of the measured and calculated resistivities is given in Fig. 3,

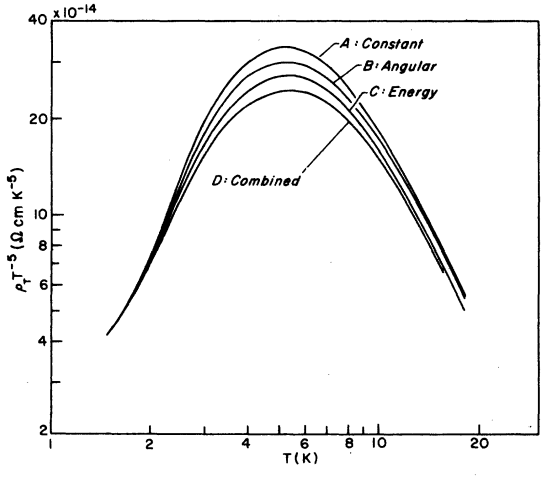

FIG. 2. Temperature-dependent electrical resistivity calculated with Bardeen's form factor for four choices of trial function: (A) $\tau(\hat{k}) =$ constant, (B) angular dependence alone (K_4 and K_6 added), (C) energy dependence alone (η^2 added), and (D) combined dependences [five nontrivial parameters—see Eq. (12)].

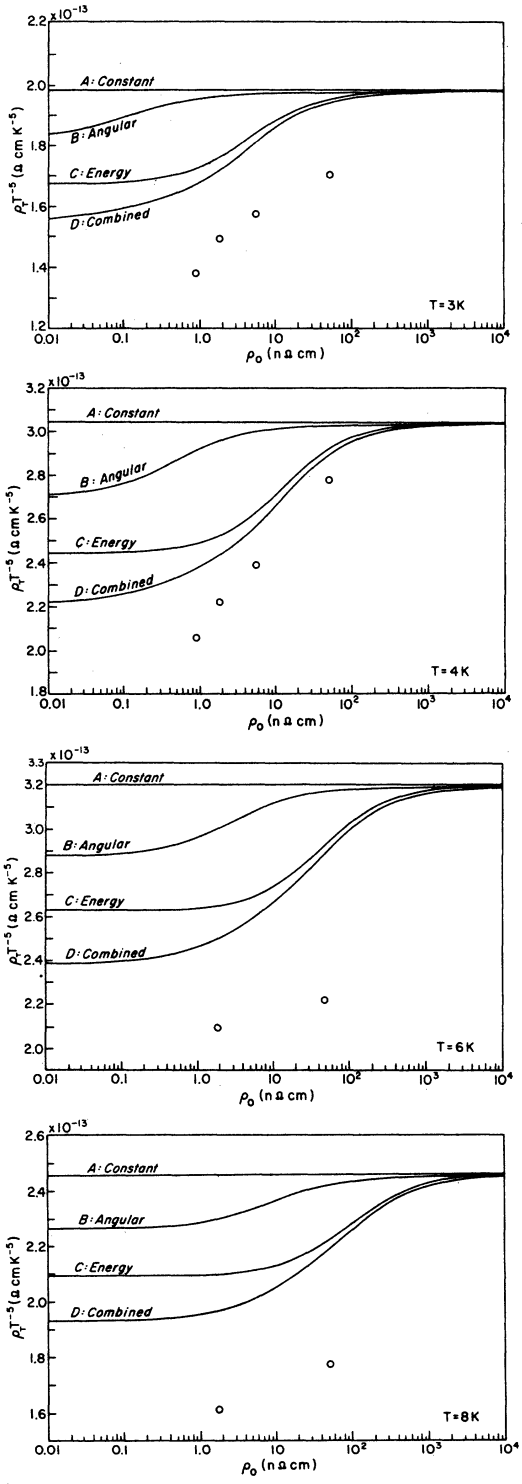

FIG. 3. Calculated and measured temperature-dependent resistivities as functions ρ_0. Calculated curves correspond in the clean limit to those shown on Fig. 2. Note that angular and energy dependences [(B) and (C), respectively] are important at different values of ρ_0. Circles correspond to samples with $\rho_0 = 55$, 5.5, 1.8, and 0.9 $n\Omega$ cm, reported in Ref. 1.

where calculated resistivities $\rho_T(T, \rho_0)$ are plotted as functions of ρ_0 at selected temperatures. These clearly exhibit the second important feature of the energy-dependent contribution—namely, that it occurs for larger values of ρ_0 than the angular-dependent one. This feature is essential for understanding the data at 3 and 4 K. Moreover, the theory predicts that still dirtier samples should exhibit further DMR near 8 K, while at 3 and 4 K the dirtiest sample shown is already quite close to saturation (i.e., to the dirty limit).

We must now discuss the sensitivity of these results to the details of the calculation. First, to the choice of form factor: the overall magnitude of the resisitivity is quite sensitive to this choice; in fact, if the Ashcroft form factor[20] were used, then the calculated resistivities would lie everywhere below the measured ones (see for example Refs. 4, 9) rather than above them as in the case of the Bardeen form factor[19] (Fig. 3). By adjusting the Ashcroft form factor within the range of the accuracy to which it may be "determined" by other measurements, one may in fact reproduce the observed magnitude of the resistivity.[9] We have done this, and the results are shown in Fig. 4. These plots demonstrate the important remaining point that DMR are not very sensitive to the functional form chosen as long as the resistivities themselves are comparable for the two choices being compared. Incidentally, the DMR are sensitive to the *magnitude* of the resistivity (or more precisely, to its umklapp component, which is most affected by the choice of form factor); the fractional DMR (i.e., Δ/ρ_T) scales roughly linearly with ρ_T. This behavior is discussed in detail in Ref. 6, and is evident in the calculations of Refs. 4 and 5 as well.

Next we must discuss the sensitivity of our results to the trial function. To do this we exploit the approximate additivity of the effects due to angular and energy dependences to examine the nature of the convergence of each expansion taken by itself. First, the Kubic harmonic expansion has been examined elsewhere,[21] and the improvement achieved by going beyond K_6 is very slight. The larger corrections obtained by including higher powers in the *energy* expansion are exhibited on Fig. 5. These corrections are small at 4 K and

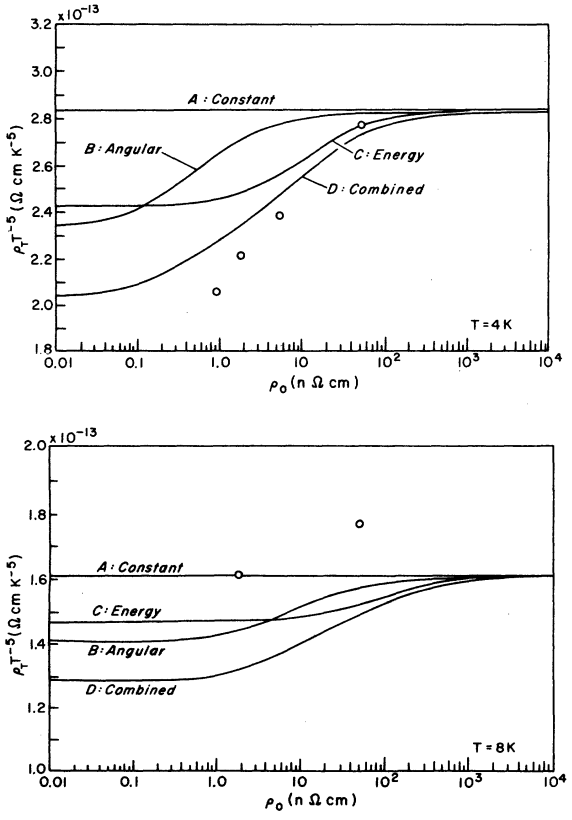

FIG. 4. Repeat of Fig. 3 with Ashcroft's form factor used in place of Bardeen's form factor. Core radius parameter R_c adjusted from Ashcroft's quoted value 1.13 to 1.16 Å to fit resistivity in magnitude. See Ref. 20.

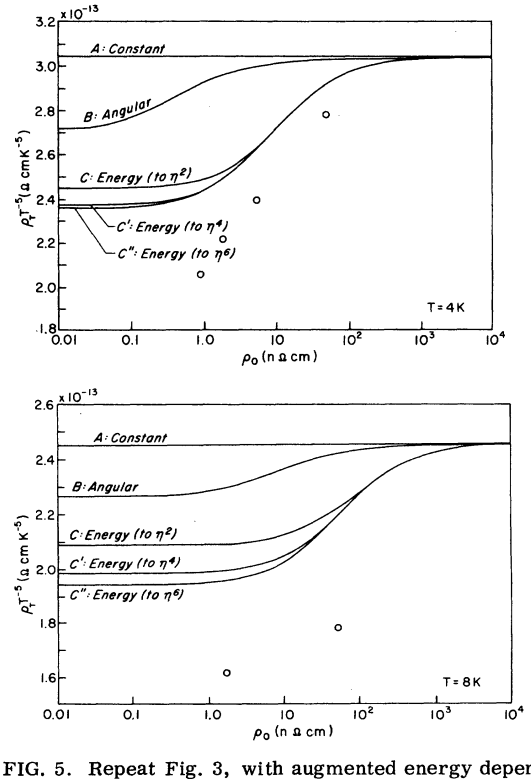

FIG. 5. Repeat Fig. 3, with augmented energy dependence in the trial function. Curves C, C', and C'' correspond to the retention of terms up to η^2, η^4, and η^6, respectively, in the energy expansion. Angular dependence is retained only in curve B. (Bardeen form factor used, as in Figs. 2 and 3).

somewhat increased at higher temperatures, but in all cases occur only at the smaller values of ρ_0. The state of agreement with the data is not altered.

Before presenting the thermal-resistivity results, we should repeat that since the angular dependence is unimportant, we can only confirm here the conclusions already reached by other authors. Perhaps it is useful nevertheless to present these results for comparison with the electrical resistivity since the calculations are parallel, and to review the state of agreement (and disagreement) with experiment for the thermal case.

First, to compare the effects of the angular and energy dependences over the temperature range of interest, we plot $W_T T^{-2}$ versus T on Fig. 6, for a series of successive improvements to the trial function. The top curve results from the simplest trial function $\tau(\vec{k}) = \text{constant}$ [or $\Psi(\vec{k}) \sim \eta\cos\theta$, see Eqs. (4), (5), (11), and (12)] and thus represents the dirty limit, $W_T(T, \infty)$ [Eq. (18)]. Ignoring the small splittings, the three remaining curves represent, in descending order, the retention of η^3, η^5, and η^7 terms in the trial function. The small splitting of the top two curves represents the inclusion of angular dependence. We find, as in the electrical case, that the effects of angular and energy dependence are (to order η^3) approximately additive, and therefore omit the (presumably small) angular-dependent corrections from the η^5 and η^7 calculations. This result confirms a previous conclusion drawn by Kus,[11] who treated angular dependence through a quite different approximation (discussed earlier) and found a similarly small effect.

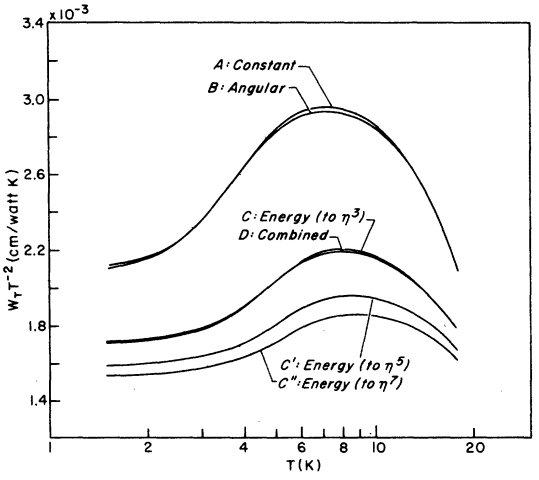

FIG. 6. Calculated temperature-dependent thermal resistivity [W_T, Eq. (18)] is shown as a function of temperature for various choices of trial function: (A) $\tau(\vec{k})$ = constant (i.e., $\psi \sim \eta\cos\theta$), (B) angular dependence alone (K_4 and K_6 added), (C) energy dependence alone (η^3 added), (D) a combination of (B) and (C) [see Eq. (12)], (C') energy expansion including η^5, (C'') energy expansion including η^7 (Bardeen form factor).

To make a comparison with the data[3] and with Leavens'[12] calculation, it is instructive to plot W_T^{-2} versus $W_0 T$ at selected temperatures, as done on Fig. 7. The solid curves represent the same trial functions shown on Fig. 6. The η^3 correction is very similar to Ekin's result (not shown). The η^5 and η^7 corrections improve the calculation in the clean limit, although Leavens' clean limit (being exact, except for the negligible angular-dependent corrections) is slightly better. Note, however, that the η^3 calculation seems to be an excellent approximation close to the dirty limit. Moreover, the maximum *slope* of the theoretical curve does not seem to be affected greatly by improvements to the trial function, beyond the η^3 term. Hence all of the calculations fail to explain the large slope exhibited by the data. Figure 7 dramatizes the conclusion that another mechanism (such as those mentioned at the beginning) is responsible

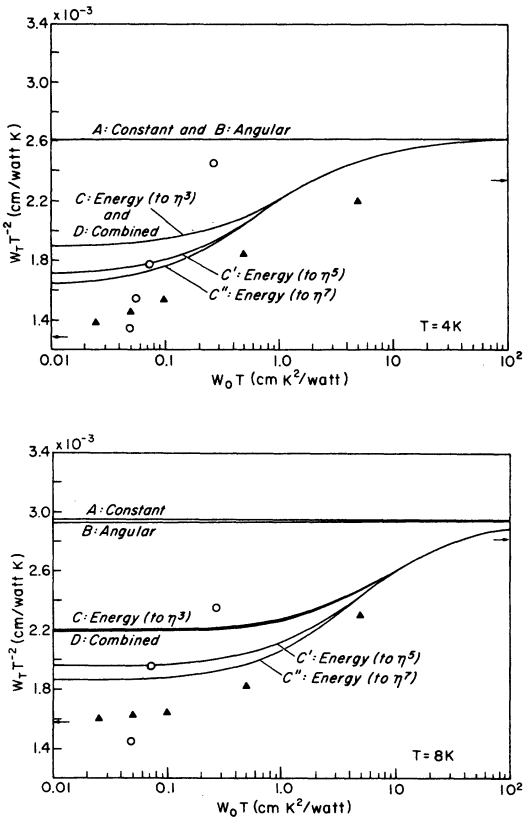

FIG. 7. Temperature-dependent thermal resistivity as a function of the "residual" resistivity $W_0 T$. Solid lines are our calculated results, corresponding to those of Fig. 6. Triangles represent calculation by Leavens (Ref. 12). Arrows near margin represent his clean and dirty limits. Circles represent data of Ref. 3.

for the observed DMR in the thermal resistivity.

It is clear on the other hand that for the electrical resistivity, no additional mechanisms need be invoked for temperatures down to 3 K.

A concluding point which is not very important for the present work, but which may have relevance for other metals with larger DMR, is the fact that the contributions from energy and angular dependence to the total improvement in the calculated resistivity are not perfectly additive. Although the departures from additivity are small in potassium, it is interesting that these departures may have either sign (i.e., the interference between the energy- and angular-dependent contributions may be either "destructive" or "constructive"). This is illustrated on Fig. 8, where we have plotted the quantity

$$\mathfrak{D}(B, C; D) = [\Delta\rho(D) - \Delta\rho(B) - \Delta\rho(C)]/\Delta\rho(D),$$

where, for example,

$$\Delta\rho(D) = \rho(A) - \rho(D)$$

is the improvement gained on going from the simplest trial function (A) to the more sophisticated one (D). Referring to Fig. 3, where (D) represents combined angular and energy dependences, and (B) and (C) represent the separate dependences, respectively, we see that $\mathfrak{D}(B, C; D)$ is a measure of the departure from additivity of the two individual improvements $\Delta\rho(B)$ and $\Delta\rho(C)$. The interesting feature of Fig. 8 is that $\mathfrak{D}(B, C; D)$ is positive somewhere, representing "constructive" interference between energy- and angular-dependent contributions. This positivity occurs at larger ρ_0 values, where the improvements $\Delta\rho(D)$, etc., are small. It is not surprising that $\mathfrak{D}$ should become negative in the region where the improvements are larger, since there would be a natural limit on additivity if the individual improvements were to approach 50%. (In such cases it would not be sensible to speak of additivities in the sense used here.) Thus the two significant features of Fig. 8 are that $\mathfrak{D}$ is generally small for potassium, and that it can in principle be positive (indicating "constructive" interference).

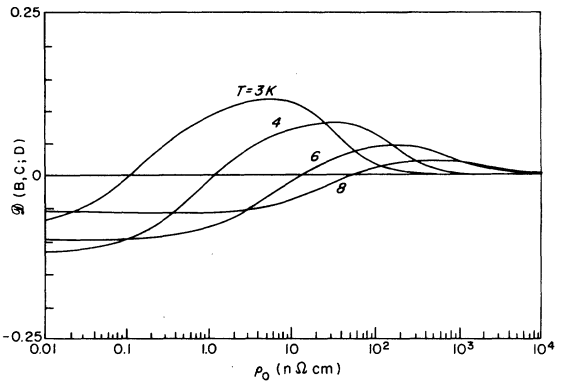

FIG. 8. Departures from additivity of the improvements (to the calculated electrical resistivities) gained from energy and angular dependences in the trial function. The quantity $\mathfrak{D}(B, C; D)$, defined in the text, is calculated from the plots on Fig. 3. The positive values occurring at larger ρ_0 values indicate that larger DMR are predicted by a trial function containing both energy and angular dependences than by the addition of the separate DMR arising from each dependence taken alone.

APPENDIX

In the text we retain only even (odd) powers of the energy variable η in the electrical (thermal) conductivity calculation. We present here a general proof that the exact deviation function $\Psi(\vec{k})$ is an even (odd) function of η at *each* angular position $\hat{k}$ on the Fermi surface. To begin, we decompose the exact function

$$\Psi(\vec{k}) = E(\hat{k}, \eta) + O(\hat{k}, \eta) \tag{A1}$$

into even and odd functions, E and O, of η. The angular dependence ($\hat{k}$) of each function may be considered arbitrary. In the resistivity functional

$$\rho\{\Psi\} = (\Psi, P\Psi)(X, \Psi)^{-2}, \tag{A2}$$

the denominator simplifies because of the evenness (oddness) of $X(\eta)$ (see 3, 4) in the electrical (thermal) case, as follows:

$$(X, \Psi) = \begin{cases} (X, E), & \text{electrical case} \\ (X, O), & \text{thermal case}. \end{cases} \tag{A3}$$

However, both even and odd components contribute to the numerator

$$(\Psi, P\Psi) = (E, PE) + (O, PO), \tag{A4}$$

while the cross term vanishes as we demonstrate shortly. Since the collision operator P is positive-definite, both terms contribute positively to the resisitivity unless one of the functions E or O vanishes identically. Since the exact $\Psi(\vec{k})$ minimizes $\rho\{\Psi\}$, it follows that O vanishes identically in the electrical case, while E vanishes identically in the thermal case.

To complete the proof we now need only show that the cross term vanishes from the numerator. Using the definitions (2), (13), and (15), we write out the cross term

$$(E, PO) = \frac{4\pi}{k_B T \hbar^3 v_F^2 (2\pi)^6} \iint d^2k\, d^2k \sum_\sigma |g_\sigma(\hat{k}, \hat{k}')|^2 \iint dE\, dE' \frac{f^0(E) f^0(E')}{|e^{-\eta} - e^{-\eta'}|}$$
$$\times [\delta(E - E' - \hbar\omega_\sigma) + \delta(E - E' + \hbar\omega_\sigma)]\, E(\hat{k}, \eta)[O(\hat{k}, \eta) - O(\hat{k}', \eta')], \tag{A5}$$

where a decomposition into energy and angular (d^2k) integrations was made, and the matrix element's exclusive dependence on the angular variables was made explicit. If the transformation $E \to -E$ and $E' \to E'$ is made, then the products EO both change sign, while the rest of the integrand remains unchanged since

$$f^0(E)f^0(E')\left|e^{-\eta}-e^{-\eta'}\right|^{-1}=f^0(-E)f^0(-E')\left|e^{\eta}-e^{\eta'}\right|^{-1}.$$

Hence the total integrand changes sign and consequently must vanish. This completes the proof.

---

*Work supported by the United States ERDA through Grant No. AT(11-1)-2315.

[1]J. W. Ekin and B. W. Maxfield, Phys. Rev. B 4, 4215 (1971).
[2]D. Gugan, Proc. R. Soc. A 325, 223 (1971).
[3]R. S. Newrock and B. W. Maxfield, Phys. Rev. B 7, 1283 (1973).
[4]J. W. Ekin and A. Bringer, Phys. Rev. B 7, 4468 (1973).
[5]F. W. Kus and J. P. Carbotte, J. Phys. F 3, 1828 (1973).
[6]W. E. Lawrence, Phys. Rev. B 12, 4161 (1975).
[7]M. Kaveh and N. Wiser, Phys. Rev. B 9, 4053 (1974).
[8]R. C. Shukla and R. Taylor J. Phys. F (to be published).
[9]P. N. Trofimenkoff and J. W. Ekin, Phys. Rev. B 4, 2392 (1971).
[10]J. W. Ekin, Phys. Rev. B 6, 371 (1972).
[11]F. W. Kus, J. Phys. F 6, 59 (1976).
[12]C. R. Leavens, J. Phys. F 7, 163 (1977).
[13]H. Van Kempen *et al.*, Phys. Rev. Lett. 37, 1574 (1976).
[14]E. H. Sondheimer, Proc. R. Soc. A 203, 75 (1950).
[15]J. E. Robinson and J. D. Dow, Phys. Rev. 171, 815 (1968).
[16]See Refs. 5 and 6 for discussions of this point.
[17]A. H. Wilson, *Theory of Metals* (Cambridge University Cambridge, England, 1958).
[18]R. A. Cowley, A. D. B. Woods, and G. Dolling, Phys. Rev. 150, 487 (1966).
[19]J. Bardeen, Phys. Rev. 52, 688 (1937); pseudopotential parameters used are the same as those of Refs. 1, 4, 9, 10, so that a meaningful comparison with their results (particularly those of 4 and 10) may be made.
[20]N. W. Ashcroft, Phys. Lett. 23, 48 (1966). In this case, the single parameter (core radius R_ϕ) is adjusted to fit magnitude of resistivity for the sake of comparing DMR with those predicted by Bardeen form factor.
[21]F. Mitchell and W. E. Lawrence (unpublished).